Metrol. Meas. Syst., Vol. 32 (2025), No. 3
DOI: 10.24425/mms.2025.154673

METROLOGY AND MEASUREMENT SYSTEMS
Index 330930, ISSN 0860-8229
www.metrology.wat.edu.pl

IMPACT OF STL FILE FORMAT ON THE CYLINDRICITY DEVIATION OF MODELS MANUFACTURED USING FDM TECHNOLOGY

Paweł Zmarzły, Paweł Szczygieł, Anna Bujarska

Kielce University of Technology, Faculty of Mechatronics and Mechanical Engineering, Tysiąclecia Państwa Polskiego 7 Ave., 25-314 Kielce, Poland (✉ *pzmarzly@tu.kielce.pl*)

Abstract

Fused Deposition Modeling (FDM) is a category of MEX additive manufacturing processes that has gained considerable popularity. Its ability to produce cylindrical machine parts makes it a particularly useful technology in this field. In order to ascertain the accuracy of the cylindrical component, it is necessary to undertake a measurement and evaluation of the cylindricity deviation. Such a measurement can identify defects that are the consequence of the 3D printing process, thus providing valuable insight into the quality of the printed object. Nevertheless, in numerous studies, the impact of the manner in which STL digital files are saved on the formation of errors in the shape of cylindrical elements is overlooked. This article presents studies aimed at determining the influence of STL recording of a virtual model on the accuracy of the printout, as determined by cylindricity deviation. The measurements were conducted utilising a Prismo Navigator coordinate measuring machine produced by Zeiss. It has been demonstrated that the manner in which a digital file is saved has an effect on the characteristics of irregularities in cylindrical surfaces, which in turn affects the value of cylindricity deviation. The findings of the study, as detailed in the article, will provide a framework for the selection of parameters for the recording of STL files, with the objective of obtaining cylindrical surfaces of an acceptable quality *i.e.* the lowest value of cylindricity deviation.

Keywords: 3D printing, FDM, MEX, cylindricity.

1. Introduction

The utilisation of additive technologies is becoming increasingly prevalent in industrial production based on ISO or ASME standards [1]. The growing prevalence and enhanced characteristics of construction materials have facilitated the integration of 3D printing in a multitude of economic sectors, including the electronics industry and the medical field [2]. In the latter, 3D printing is employed in the fabrication of prostheses, implants, and personal protective equipment [2, 3]. The necessity to reduce costs and produce the highest quality goods requires the parameters of the *stereolithography* or *standard tessellation language* (STL) file to be adjusted in order to ensure the smallest possible shape errors and desired mechanical properties are achieved during the printing process [4]. Additive manufacturing is a method of creating a three-dimensional object by layering materials according to a digital model created using *computer-aided design* (CAD) software. The PN-EN ISO/ASTM 52900 [5] standard defines various categories of additive manufacturing, including bonding of powdered material with liquid *binder jetting* (BJT), *vat photopolymerization* (VPP) or the most popular layer extrusion of *material extrusion* (MEX). The final category comprises *fused deposition modeling* (FDM), *fused filament fabrication* (FFF) and *layer plastic deposition* (LPD) technologies. The study described in this article will be carried out using FDM technology.

Fused deposition modeling technology was first developed in the late 1980s. At the present time, this is the most prevalent method of 3D printing. The process is most commonly referred

Article history: received December 23, 2024; revised February 23, 2025; accepted May 22, 2025; available online July 11, 2025.

to as "3D printing of plastic." The design of the printed model should be done using 3D modelling software CAD programs. It is a prerequisite that the program is capable of saving the model in STL format, whereby the model is represented as a mesh of triangles in three-dimensional space. In FDM technology, the models are constructed using filaments (plastics for the formation of diverse geometries via the application of elevated temperatures, typically within the range of 190°C to 260°C, in the majority of 3D printers). The print head is positioned in such a way that it moves in an XY plane, with the X-axis representing the movement of the head and the Y-axis representing the movement of the work table. Once the initial layer has been deposited, the worktable is lowered in the Z-axis direction, or alternatively, the head is elevated in the Z-axis direction, allowing the next layer of the 3D model to be applied. The precise action depends on the design of the 3D printer in question. Prior to the application of an additional layer to the pre-existing printed one, it is essential that the latter undergoes a cooling and hardening process. In this manner, a spatial model of the element is constructed in a gradual, additive process. A distinctive feature of this additive technology is the necessity for the utilisation of supports, namely load-bearing structures that are constructed concurrently with the model or support material. It is essential to provide support for any component that features overhangs or is suspended in the air. The utilisation of supports enables the printing of geometrically intricate shapes; however, the removal of these supports can prove challenging [6, 7]. The authors [6] pointed out that optimizing the printing process can result in improved mechanical properties such as tensile strength, fatigue strength and tribological properties. Since 3D printing, it can be used to develop different surface textures for various friction and wear applications, as well as in robotics applications for gripping.

Digital models saved in STL format are three-dimensional solids whose surfaces are composed of triangles. The most basic solid that can be described in this way can be considered a tetrahedron, composed of four triangles each of which is also a whole wall. An alternative model is that of a cuboid, in which each of the rectangular walls is constructed from two triangles. In this article, shape of the test model is taken from ISO/ASTM 52902 [8]. This standard provides a general description of the geometry of reference samples used to assess the accuracy of manufacturing elements using selected 3D printers. The present standard does not provide detailed specifications regarding the measurement parameters and sampling strategies. This applies to both contact and optical methods [9, 10].

The objective of the research presented in this article is to analyse the impact of the STL digital file on the value of shape errors, as represented by the cylindricity deviation of the 3D printed models. There are a lot of methods used to measure roundness and cylindricity [11, 12]. It should be noted that excessive values of cylindricity deviation have the potential to cause vibrations in elements that are subjected to rotational movement, or to result in assembly issues, such as those observed in screw joints [13]. The analysis of shape errors is the subject of a substantial body of research [14, 15]. Work [14] contains a detailed analysis of cylindrical elements by measuring the cylindricity and surface roughness. It has been demonstrated that the measurement parameters have a significant impact on the values of the surface roughness and cylindricity parameters. The authors of [15] investigated the dimensional accuracy and quality of the surface layer of parts produced by 3D printing. The findings indicated that the orientation of the print has a significant impact on the quality of the finished product. In work [16], the authors examined the possibility of using direct metal laser melting technology to produce cutting tools – drills. The quality of holes drilled in polyamide PA6 was evaluated using a printed drill, taking into account the variable cutting parameters. The shape of the holes was analysed in terms of its roundness, cylindricity and straightness. It has been demonstrated that *direct metal laser melting* (DMLM) technology can be effectively employed for the fabrication of prototype drills. The subject raised in article [17] concerns the assessment of errors in the shape of the crankshafts of large marine engine using measuring systems used directly in industrial conditions. It has been demonstrated that the choice of support method has a significant impact on the accuracy of measurements taken of large cylindrical objects.

The rapid prototyping standard has undoubtedly become the *Standard Tessellation Language* (STL) file. It is made up of a series of connected triangles that describe the surface geometry of an object or a 3D model. As a result, the more complex the design, the more triangles used and the higher the resolution. This also has the effect of a greater load on the software memory used for the mesh generation. The representation of the 3D solid is the triangular mesh generated by tessellation of its boundary surface. In engineering applications, this mesh needs to contain information about which side of the triangle is on the inside of the solid. The STL file is thus a representation of the triangular surface in which the vertices of each triangle are ordered to fulfil this requirement [18]. ISO/ASTM 52950 *additive manufacturing – General principles – Overview of data processing* [19] specifies the recording formats used in 3D printing technology STL is the most commonly used format for transferring data. It is a system-neutral format for the exchange of pure geometric data. It uses triangles and their normal vectors to describe the boundary surfaces of volumetric models.

In the literature, one can find studies on the identification and analysis of common errors [20] that can occur when working with files of this format and defining key criteria for assessing the geometric quality of the mesh. Studies to modify the triangle meshes to optimize print quality have been carried out in subsequent publications [18], [21, 22]. The paper [18] presents a method of detecting defects in surface mapping by constructing a multiwall data structure from an STL file. In [21], however, a surface-based modification algorithm is presented, which, adaptively and locally, increases the density of the STL model's facets. The Surface-based Modification Algorithm is an error minimising approach to locally modify the STL mesh based on chord error, cusp height and cylinder error for cylindrical features and is typically able to achieve a smaller file size compared to the Unified Export option. The aim of the method proposed [22] is to show the possibility of generating adaptive surface meshes suitable for the finite element method, directly from an approximate boundary representation of an object created with CAD proving that not using the parametric representation of the geometric model allows to override some of the limitations of conventional meshing software that is based on an representation of the geometry.

In most of the research papers, the authors focus on assessing the influence of technological parameters, type of material, postprocessing on the quality of manufactured parts. In connection with the emergence of new guidelines contained in [8], which concern the method of 3D printing and measurement of selected geometric features, the paper assesses the impact of digital file recording on the value of cylindricity deviation of cylindrical elements. In [23] it was pointed out that changing the STL mesh shaping algorithm or modifying it afterwards can have a beneficial effect on the quality of 3D printing.

The studies presented in this article provide guidelines for the selection of parameters for recording an STL file in order to obtain cylindrical elements with the least cylindricity deviation. In addition, the recommended strategy for measuring this type of shape deviation is indicated.

2. Materials and Methods

The research procedure contain a few steps. The procedure began with designing samples in selected CAD software. At this stage, digital 3D models were created and then exported to the STL format for further processing in 3D printing technology. The next step involved importing STL files into 3D printer software and manufacturing samples using 3D printing. Once printed, the samples underwent cylindricity measurements. Subsequently, the samples were subjected to macroscopic observations to assess their surface quality and detect potential surface defects. The flow char of research procedure is presented in Fig. 1.

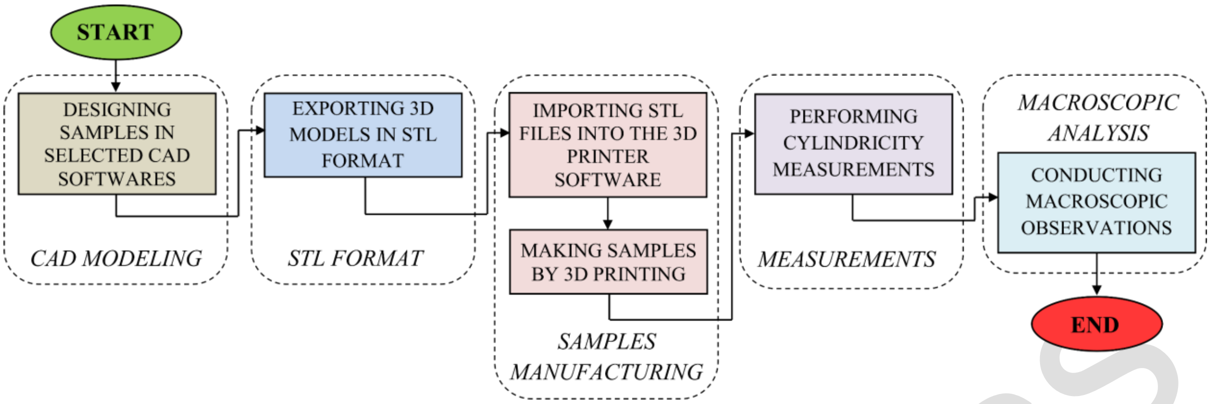

Fig. 1. Flow chart of research procedure.

2.1. Materials

The material used in the study was *polylactic acid* (PLA) with a density of 1.24 g/cm^3 in the form of a 1.75 mm diameter filament with the trade name Fiberlogy easy PLA (*Fiberlab*, Brzezie, Poland). Table 1 shows selected mechanical properties.

Table 1. Selected mechanical properties [24].

Mechanical properties	Test Method	Unit	Value
σ_y	ISO 527	MPa	50
σ_b	ISO 527	MPa	53
E	ISO 527	MPa	3500
ε_y	ISO 527	%	6
σ_f	ISO 178	MPa	81
E_f	ISO 178	MPa	3800

2.2. Research model

The samples were designed in accordance with [8] in *SOLIDWORKS* (Dassault Systèmes, Vélizy-Villacoublay, France) and in *Siemens NX* (Siemens, Munich, Germany). The programs use from their own algorithms to convert the model to STL format. In this article, the STL mesh arrangement in program *SOLIDWORKS* is referred to as Method 1, while the STL mesh arrangement in program *Siemens NX* is designated as Method 2.

Most CAD software environments allow the 3D model to be saved in STL save format, with controlled Deviation and Angle parameters, for example *FreeCAD*, Fusion [25, 26]. However, it should be noted that these programs can perform the triangulation operation with different algorithms. In addition, *SOLIDWORKS* and *Siemens NX* are the programmes most commonly used in the industrial environment, so this approach seems appropriate in practical terms. In the future, it is planned to extend the research to other software with different triangulation algorithms than those presented in this article.

Figure 2 shows the geometry of the sample, consisting of two concentric rings that are closely spaced together. The concentric rings are centred on a thin circular plate. A *medium* variant sample was used.

DOI: 10.24425/mms.2025.154673

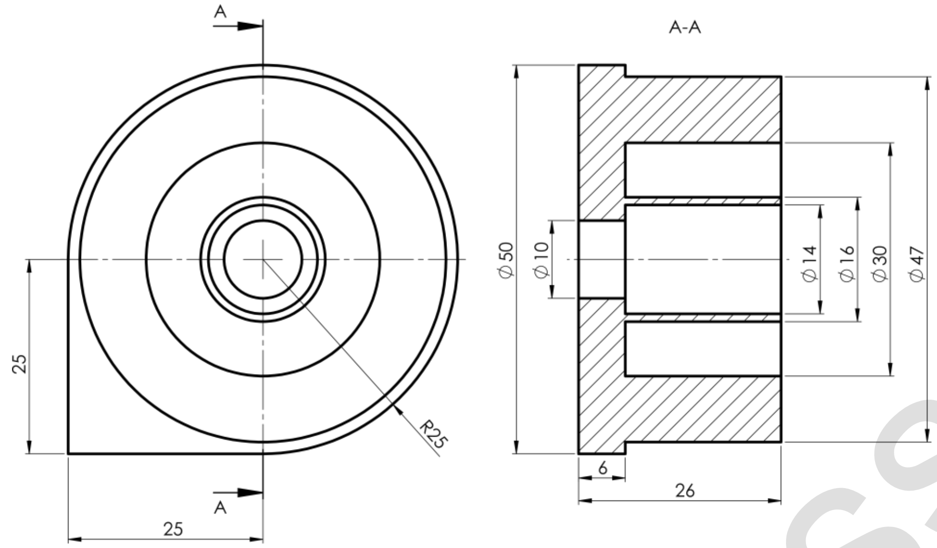

Fig. 2. Medium sample dimensions [8].

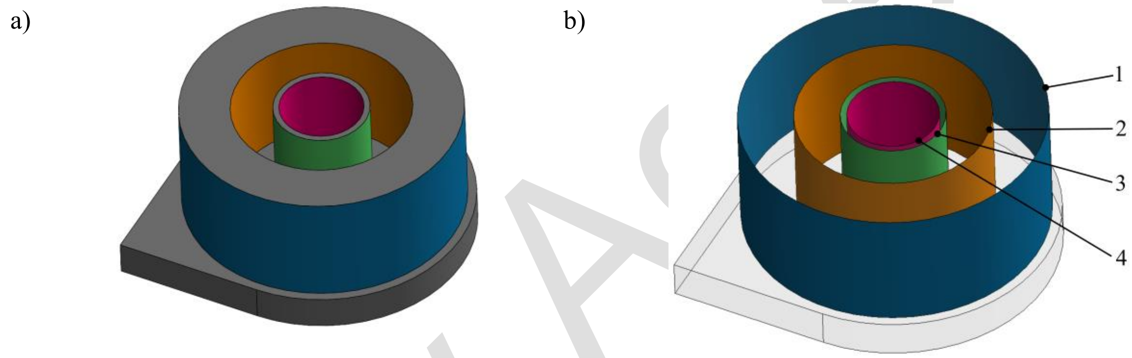

Fig. 3. CAD model view: (A) full; (b) excluding the top surface to show the measured surface, where: 1 - surface 1, 2 - surface 2, 3 - surface 3, 4 - surface 4.

The samples were saved in STL format (the surface was described using triangles). The mesh parameters are included in Table 2.

Table 2. Mesh parameters.

Method	**Deviation Tolerance, mm**	**Angle Tolerance, °**	**Number of triangles**
1	±0.01	±1	8288
2	±0.01	±1	8288

Figure 4 shows the mesh views of the models in which the Fig. 4a and Fig. 4b represent the meshes obtained successively by Method 1 and Method 2, while Fig. 4c shows the differences resulting from the mesh arrangement for Methods 1 and 2.

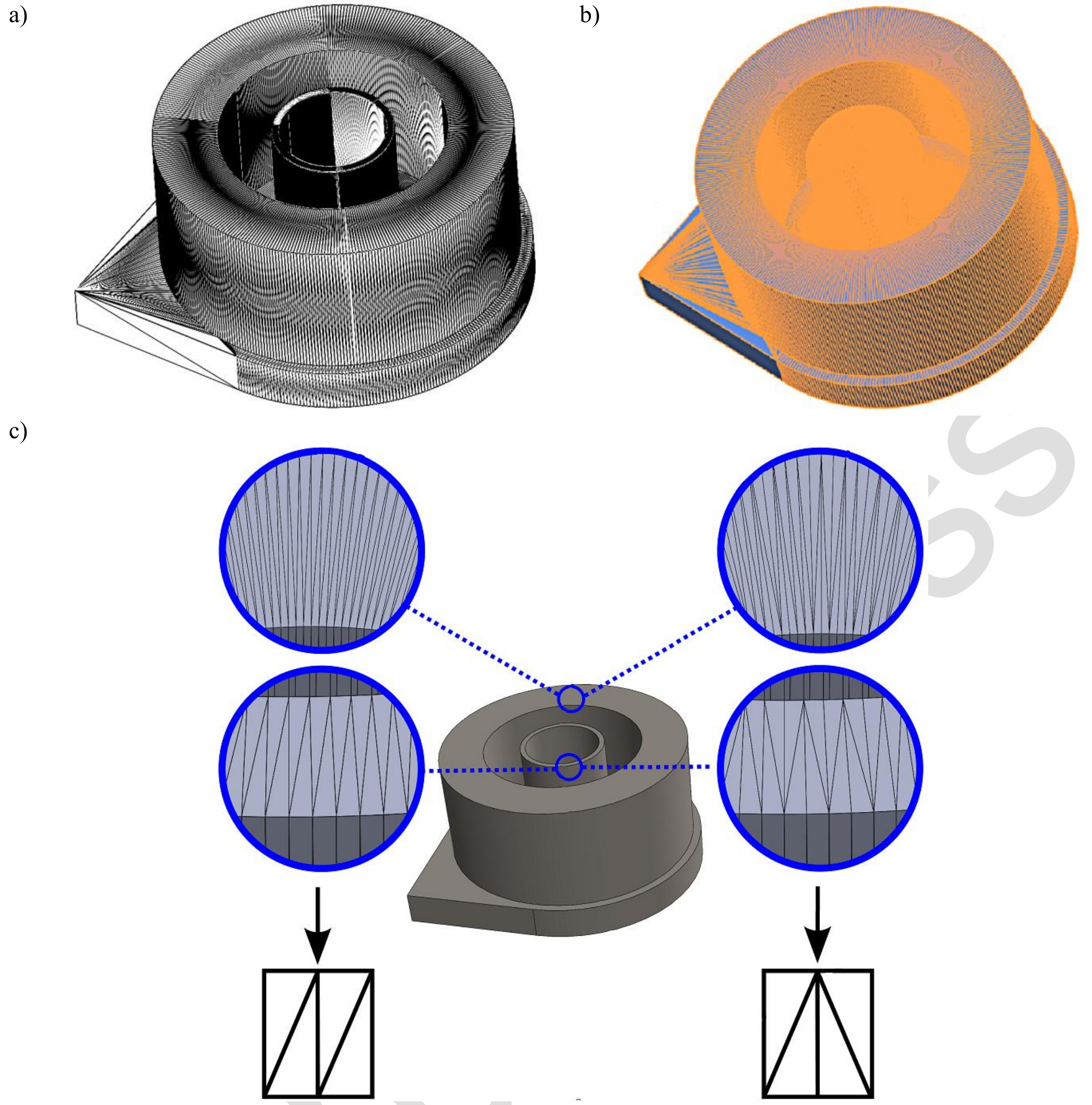

Fig.4. STL mesh: a) obtained using Method 1, b) obtained using Method 2, c) comparison of the methods.

On the basis of the mesh view shown in Figure 4, it can be observed another way in which the methods under analysis can be interlinked. In Method 1, the individual facets resemble rectangular triangles, while in Method 2, the facets resemble isosceles triangles. It should be added that there is a difference in the density of the triangles depending on the surface selected, which can have an effect on the quality of the print surface.

2.3. 3D printing technology

In order to produce the samples, FDM/FFF 3D printing technology, which falls under the category of MEX according to [5], was used. This technology involves extruding a thermoplastic material through a heated nozzle. The material in a semi-liquid state is applied to the printer's work table (bed) and a 3D model is then built layer by layer. A 3D printer MakerBot Sketch machine (*MakerBot*, USA, New York) was used. According to the manufacturer, the chemical composition of the material is >98% polyactide, plus filler and functional additives [27]. The 3D printing parameters are included in Table 3.

Metrol. Meas. Syst., Vol. 32 (2025), No. 3
DOI: 10.24425/mms.2025.154673

Table 3. 3D printing parameters.

Parameter	Unit	Value
Extruder temperature	°C	220
Bed temperature	°C	65
Shell	–	2
Layer Height	mm	0.1
Printing pattern	–	Linear
Infill density	%	50

Based on the digital STL models obtained by Methods 1 and 2, a number of samples were produced for measurements. Two series of samples were used for the study. The first (produced using method A) and the second (produced using method B) series consisted of 10 samples. A total of 20 samples were produced. However, the results of the measurements presented should be regarded as statistical values from the series of measurements. Photographs of printed samples are shown in Fig. 5.

a)

b)

Fig.5. Photograph of the actual models: A) Method 1, b) Method 2.

2.4. Measurement of cylindricity

According to PN-EN ISO 1101:2017-05 cylindricity deviation (ΔC) is the largest distance between points on the actual surface and the surface of the reference cylinder that is tangential to the area of the partial zone. A reference cylinder is the one with the smallest diameter inscribed on the surface of the shaft or the one with the largest diameter circumscribed to the surface of the hole. The tolerance zone boundary is formed by two coaxial cylinders with radii differing by a value t from the specified permissible tolerance for this deviation. Previous practice has shown that the most straightforward cylinder to define is the associated cylinder determined using the least squares method. The parameter determined relative to this cylinder is defined as CYL_t. It is the sum of the largest positive absolute value and the largest negative local cylindricity deviation, both measured relative to the associated cylinder determined by the least squares method, as defined by the formula:

$$CYL_t = CYL_p + CYL_v \tag{1}$$

where: CYL_p the value of the largest positive local cylindricity deviation measured relative to the reference cylinder, which is determined using the least squares method; CYL_v the absolute value of the largest negative local cylindricity deviation relative to the reference cylinder, also determined using the least squares method.

Active or passive scanning probe heads are used to carry out specialised measurements with the *coordinate measuring machine* (CMM). In the case of using impulse heads, the measurement time and selection of the optimal number of measuring points become a problem, because it is the adopted number of points that will depend, among others, on the error of assessing the cylindricity profile [29]. As a result, the study uses the Zeiss VAST Gold (Zeiss, Oberkochen, Germany) scanning head, which enables scanning at different speeds even at very high values (up to 300 mm/s) thanks to the use of Navigator system. The accuracy of form error measurement on the CMM is increased by the use of active scanning heads. To assess the cylindricity deviation of precision machine parts, *e.g.* rolling bearing components, it is recommended to use specialised measuring systems based on the method of measuring radius changes. Due to the relatively large values of cylindricity deviations of parts made using additive MEX technologies, the use of a coordinate measuring technique for such assessment is sufficient.

The *Zeiss Prismo Navigator* coordinate measuring machine and *Zeiss Calypso* software (*Zeiss*, Oberkochen, Germany) were used for the measurements. Measurements were carried out under controlled conditions at an ambient temperature of 20°C. The parameters listed in Table 4 characterise the selected measuring machine.

Table 4. Coordinate Measuring Machine Parameters.

Parameter	**Value**
Measurement range	X = 900 mm; Y = 1200 mm, Z = 700 mm
Max. permissible error/spindle error	0.9 + (L / 350) μm

The measurements were carried out using a precision styli with 3 mm diameter ruby sphere – a ruby sphere of the smallest possible diameter was used due to the nature of the irregularities occurring on the surface of the elements to be measured, to reduce the possibility of mechanical filtration.. The sampling step size was 0.05 mm. Two measurement speeds were used depending on the diameter dimension of the sample surface. Surfaces 1 and 2 (Figure 3b) were measured at 10 mm/s. Surfaces 3 and 4 were measured at 5 mm/s. Due to the values of the cylindricity deviation, these are typical stylus feed rates when measuring form deviations on the CMM.

In this research, the probe was not qualified by the dynamic tensor method, so in order to maintain the same sampling level for all surfaces, it was necessary to reduce the scanning speed for smaller diameters.

3. Results

In order to determine the cylindricity deviation, the measured profiles were filtered with a Gaussian filter in the range of 2-50 UPR, which allows the analysis of the waviness components in addition to the shape error. The deviation was determined on the basis of the reference cylinder, the so-called medium cylinder, determined by the method of least squares. The results of the measurements of the cylindricity parameter are presented in Table 5 and

DOI: 10.24425/mms.2025.154673

Fig. 6, where the surfaces correspond to those indicated in Figure 3b, while the obtained values characterize the parameter CYL_t.

Table 5. Measurement results.

Surface No.	Method 1		Method 2	
	$\bar{x}$, mm	SD, mm	$\bar{x}$, mm	SD, mm
1	0.1792	0.0330	0.2475	0.0485
2	0.1425	0.0126	0.1847	0.0212
3	0.1353	0.0401	0.1820	0.0374
4	0.1142	0.0234	0.1915	0.0188

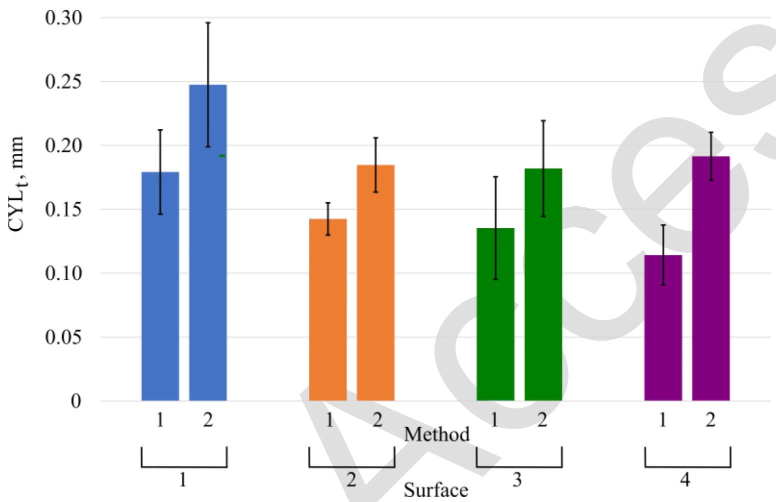

Fig. 6. Measurement results.

Analysing the results of the measurements presented in Table 5 and Fig. 6, it can be concluded that the method of saving the STL file has a significant impact on the cylindricity deviation values of surfaces of models manufactured using FDM technology. Higher cylindricity deviations were observed for all examined cases for models produced using Method 2. The largest differences in cylindricity deviations were recorded for surface '4,' which represents the hole of the bushing with the smallest diameter. Therefore, it can be concluded that the cylindricity of holes with smaller diameters depends on the method used to save the digital STL file. A comprehensive analysis of the measurement results revealed that the largest cylindricity deviation values were obtained for the outer surface of the samples (for both models produced using Method 1 and Method 2). Moreover, for this surface, the highest standard deviation values were calculated, indicating a significant disparity in the cylindricity deviations measured for the individual samples. The results presented in the table indicate that an increase in the diameter of the sampled surfaces leads to an increase in the cylindricity deviation. Additional tests were carried out, which allowed to determine the repeatability of measurements at EV=0.394 mm.

In order to evaluate the nature of the surface irregularities of the cylindrical surfaces, Figs. 7 and 8 present the profiles of cylindricity for the individual surfaces of selected samples manufactured using FDM technology, based on digital files saved using both Method 1 and Method 2.

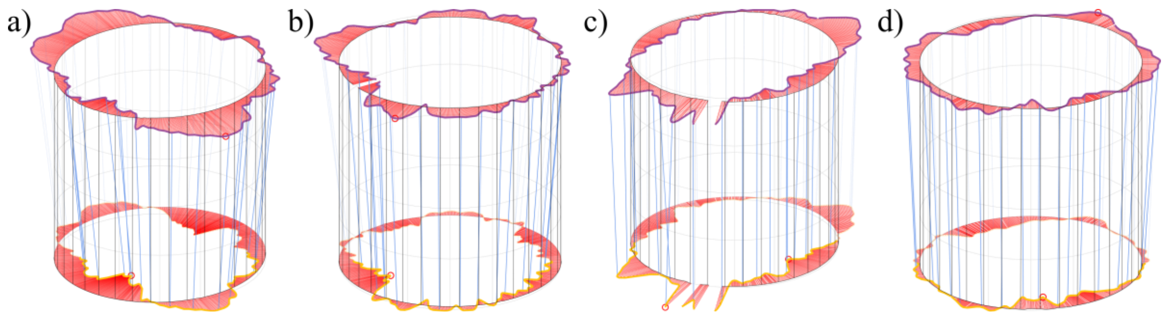

Fig.7. Cylindrity profiles of the surface of samples manufactured using Method 1:
a) Surface 1, b) Surface 2, c) Surface 3, d) Surface 4.

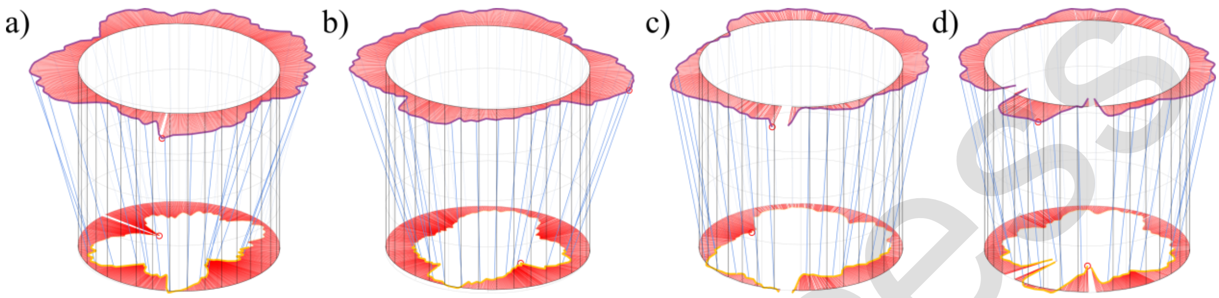

Fig. 8. Cylindrity profiles of the surface of samples manufactured using Method 2:
a) Surface 1, b) Surface 2, c) Surface 3, d) Surface 4.

In assessing the cylindricity character of the measured surfaces shown in Fig. 7 (digital files recorded using Method 1), the presence of ovality was noted, particularly on the outer surface of the model with the largest diameter (Fig. 3a and Fig. 7a). However, when assessing the results of the cylindricity profile measured on the samples produced from the digital file recorded by Method 2 (Fig. 8), a clear conicity can be observed in addition to ovality. In both recording Methods 1 and 2, ovality may be the result of the formation of the so-called "seam", which is related to the initial location of the overlap of individual layers of material. On the other hand, the visible conicity can result from the specific way of bonding and cooling each layer of the material. There may be "blending" of the layers on the outer surfaces, which can be seen as an increase in the model's diameter with each successive layer being applied. It should be noted that for Method 2, higher cylindricity deviation values were recorded for all examined surfaces.

In order to better illustrate the characteristics resulting from the digital STL file format, additional microscopic measurements were made using the MAHR vision MN320 (*Mahr*, Göttingen, Germany) digital microscope, with an optical magnification of X1 and reflected light. Views of the measured surfaces are shown in Fig. 9, where the outline of the STL file is additionally marked.

Analysing the macroscopic views shown in Figure9, it is possible to see the visible traces of the individual layers of material applied, together with their directionality. In Method 1, the individual layers of material are similar in shape to rectangular triangles, while in Method 2 they are similar to an isosceles triangle. This is in line with the nature of the triangle mesh in Fig. 4. In addition, surface 1 in particular shows the refraction of cylindrical profiles. These are similar to the irregularities of the saved digital STL file. Both samples made from digital files recorded using Method 1 and Method 2 show this phenomenon.

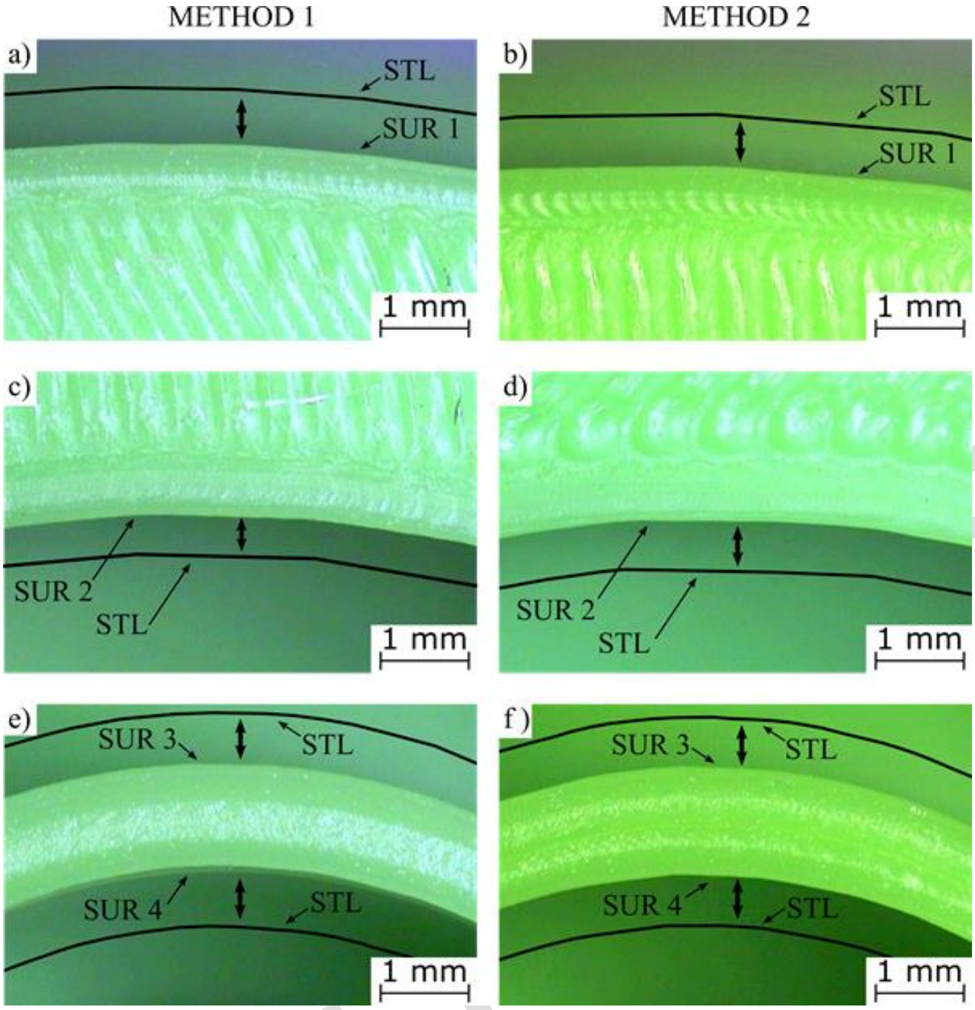

Fig. 9. Macroscopic view of the outline of the sample surfaces: a) method 1, surface 1; b) method 2, surface 1; c) method 1, surface 2; d) method 2, surface 2; e) method 1, surface 3 and 4; f) method 2, surface 3 and 4.

Analysing the macroscopic views shown in Figure9, it is possible to see the visible traces of the individual layers of material applied, together with their directionality. In Method 1, the individual layers of material are similar in shape to rectangular triangles, while in Method 2 they are similar to an isosceles triangle. This is in line with the nature of the triangle mesh in Figure4. In addition, surface 1 in particular shows the refraction of cylindrical profiles. These are similar to the irregularities of the saved digital STL file. Both samples made from digital files recorded using Method 1 and Method 2 show this phenomenon.

3.1. Discussion

In the article [30] the effect of the diameter of the printing nozzle on the cylindricity deviation was investigated. The results showed that the smallest cylindricity deviation was obtained for a nozzle size of 0.4 mm and its average value was 0.0700 mm, with a printed piece diameter of 10 mm. In this paper, such a printing nozzle diameter was also used and the smallest value obtained was 0.1142 mm, for a diameter of 14 mm. This confirms the relationship that the smaller the diameter of the component, the smaller the cylindricity.

Wolf *et al* [31] checked the effect of different printer drive systems on cylindricity deviation. The tested cylinder had a diameter of 7.5 mm and was made of PLA material and the average value of the cylindricity deviation was (for the stepper motor) 0.1055 mm. The 3D printer used for the research in this article is also equipped with a stepper motor. This again confirms that the diameter of the part has a direct effect on the cylindricity deviation.

4. Conclusion

3D printing is becoming more widespread as additive manufacturing technologies continue to develop. Initially, 3D printing was only used to create mock-ups and prototypes. These were used to give a visual representation of the final product. Today, fully functional machine parts can be produced using additive technologies. Therefore, you should be on the lookout for treatments aimed at increasing the accuracy of the elements produced by means of 3D printing. Most of the research work is focused on the evaluation of types of building materials or technological parameters on parameters describing the accuracy of prints or their mechanical properties. However, there is a limited amount of research into the influence of the parameters used to capture the digital STL file on the quality of the printed elements. This is important because the saving of a digital file is the first step in the printing process. This article assesses the impact of digital STL file storage methods on the quality of cylindrical surfaces using the two most popular CAD software.

Analysis of the results allows to draw the following conclusions:

1) The results of the research presented in the article showed the visible effect of the way in which the STL file was stored on the cylindricity deviation values. The meshes of the STL model were created differently depending on the method of saving the file. In the Method 1 the rectangular triangles were dominant, whereas in the Method 2 the equilateral triangles were dominant (Fig.4).
2) Microscopic analysis of the models showed that the way the triangle mesh was stored in the STL file was replicated in real models (Fig. 9).
3) The cylindricity profiles were characteristic curves (Fig. 7, 8). In addition, the *CYLt* cylindricity deviation itself depended on the type of digital file storage method. The difference was more than 40 % in some surfaces (Fig. 6).
4) For both the first and second method of saving the STL file, it was noted that with the increase in the diameter of the printed cylindrical surfaces, the value of the *CYLt* cylindricity deviation increased. For Method 1, the difference between the mean value of the cylindricity deviation of the No. 1 surface (the one with the largest diameter) and the No. 4 surface (the one with the smallest diameter) was about 57 %. And for Method 2, the difference was approximately 29 %.
5) When the contours of the cylindricity stock were evaluated, it was found that ovality and conicity were present, which is a direct result of the way the layers are combined in FDM technology. Research has shown that the use of scanning CMM probes can detect defects resulting from the process of combining individual layers of material in FDM technology (Fig. 7, 8).
6) Taking the smallest cylindricity deviation values as a criterion, Method 1 should be selected.

As a direction for further research, the authors will assess the impact of digital file recording in other additive technologies, such as PolyJet Matrix or Selective Laser Sintering. It also evaluates other geometric deviations such as flatness. In addition, work is being carried out on the optimization of a triangle mesh in order to have models with minimal shape deviations.

Appendices

Table 6. Nomenclature.

Nomenclature	Description
σ_y	Tensile Strength at Yield
σ_b	Tensile Strength at Break
E	Tensile Modulus
ε_y	Extension at Yield
σ_f	Flexural Strength
E_f	Flexural Modulus
FDM	Fused Deposition Modeling
MEX	Material Extrusion
STL	Standard Tessellation Language
CAD	Computer Aided Design
FFF	Fused Filament Fabrication
ΔC	Cylindricity deviation
CYL_t	It is the sum of the largest positive absolute value and the largest negative local cylindricity deviation, both measured relative to the associated cylinder determined by the least squares method
CYL_p	The value of the largest positive local cylindricity deviation measured relative to the reference cylinder, which is determined using the least squares method
CYL_v	The absolute value of the largest negative local cylindricity deviation relative to the reference cylinder, also determined using the least squares method
CMM	Coordinate Measuring Machine
$\overline{x}$	Mean
SD	Standard Deviation

References

[1] Humienny, Z., & Zdrojewski, P. (2023). ISO GPS and ASME GDT standards – differences and similarities in definitions of measurands. *Metrology and Measurement Systems*, 791–808. https://doi.org/10.24425/mms.2023.147954

[2] Espera, A. H., Dizon, J. R. C., Chen, Q., & Advincula, R. C. (2019). 3D-printing and advanced manufacturing for electronics. *Progress in Additive Manufacturing*, *4*(3), 245–267. https://doi.org/10.1007/s40964-019-00077-7

[3] Advincula, R. C., Dizon, J. R. C., Chen, Q., Niu, I., Chung, J., Kilpatrick, L., & Newman, R. (2020). Additive manufacturing for COVID-19: Devices, materials, prospects, and challenges. *MRS Communications*, *10*(3), 413–427. https://doi.org/10.1557/mrc.2020.57

[4] Petruse, R. E., Simion, C., & Bondrea, I. (2024). Geometrical and dimensional deviations of Fused Deposition Modelling (FDM) Additive-Manufactured Parts. *Metrology*, *4*(3), 411–429. https://doi.org/10.3390/metrology4030025

[5] PN-EN ISO/ASTM 52900:2022-05. (2022). Additive manufacturing — General principles — Fundamentals and vocabulary.

[6] Shahrubudin, N., Lee, T., & Ramlan, R. (2019). An overview on 3D printing technology: technological, materials, and applications. *Procedia Manufacturing*, *35*, 1286–1296. https://doi.org/10.1016/j.promfg.2019.06.089

[7] Rouf, S., Raina, A., Haq, M. I. U., Naveed, N., Jeganmohan, S., & Kichloo, A. F. (2022). 3D printed parts and mechanical properties: Influencing parameters, sustainability aspects, global market scenario, challenges

and applications. *Advanced Industrial and Engineering Polymer Research*, *5*(3), 143–158. https://doi.org/10.1016/j.aiepr.2022.02.001

[8] PN-EN ISO/ASTM 52902:2024-01. (2024). Additive manufacturing - Reference samples - Assessment of geometric accuracy of additive manufacturing systems.

[9] Nowakowski, M., Kurylo, J., & Dang, P. H. (2024). Camera Based AI Models Used with LiDAR Data for Improvement of Detected Object Parameters. In *Lecture notes in computer science* (pp. 287–301). https://doi.org/10.1007/978-3-031-71397-2_18

[10] Gogolewski, D. (2022). Multiscale assessment of additively manufactured free-form surfaces. *Metrology and Measurement Systems*, 157–168. https://doi.org/10.24425/mms.2023.144393

[11] Jermak, C. J., & Rucki, M. (2016). Static characteristics of air gauges applied in the roundness assessment. *Metrology and Measurement Systems*, *23*(1), 85–96. https://doi.org/10.1515/mms-2016-0009

[12] Poniatowska, M., & Werner, A. (2010). Fitting spatial models of geometric deviations of Free-Form surfaces determined in coordinate measurements. *Metrology and Measurement Systems*, *17*(4), 599–610. https://doi.org/10.2478/v10178-010-0049-x

[13] Grzejda, R. (2016). Modelling nonlinear preloaded Multi-Bolted systems on the operational state. *Engineering Transactions*, *64*(4), 525–531. https://doi.org/10.24423/engtrans.738.2016

[14] Zaborski, A., & Winczek, J. (2020). Imaging and computer analysis in the shape error measurements and in the cylindrical objects stereometry. *IOP Conference Series Materials Science and Engineering*, *776*(1), 012077. https://doi.org/10.1088/1757-899x/776/1/012077

[15] Chand, R., Sharma, V. S., Trehan, R., Gupta, M. K., & Sarikaya, M. (2022). Investigating the dimensional accuracy and surface roughness for 3D printed parts using a multi-jet printer. *Journal of Materials Engineering and Performance*, *32*(3), 1145–1159. https://doi.org/10.1007/s11665-022-07153-0

[16] Nowakowski, L., Skrzyniarz, M., Blasiak, S., Rolek, J., Vasileva, D., & Avramova, T. (2023). Analyzing the potential of drill bits 3D printed using the direct metal laser melting (DMLM) technology to drill holes in polyamide 6 (PA6). *Materials*, *16*(8), 3035. https://doi.org/10.3390/ma16083035

[17] Nozdrzykowski, K., Grządziel, Z., Grzejda, R., & Stępień, M. (2023). Determination of Geometrical Deviations of Large-Size Crankshafts with Limited Detection Possibilities Resulting from the Assumed Measuring Conditions. *Energies*, *16*(11), 4463. https://doi.org/10.3390/en16114463

[18] Szilvśi-Nagy, M., & Mátyási, G. (2003). Analysis of STL files. *Mathematical and Computer Modelling*, *38*(7–9), 945–960. https://doi.org/10.1016/s0895-7177(03)90079-3

[19] PN-EN ISO/ASTM 52950:2021-07. (2021). Additive manufacturing — General principles — Overview of data processing

[20] Husiev, O., & Nikiforova, T. (2022). Research of the converting stages for the volume model of the product into the control code for a 3D printer in the context of automated construction of 3D printing technology. *Ukrainian Journal of Civil Engineering and Architecture*, *4*, 38–45. https://doi.org/10.30838/j.bpsacea.2312.250822.38.876

[21] Zha, W., & Anand, S. (2015). Geometric approaches to input file modification for part quality improvement in additive manufacturing. *Journal of Manufacturing Processes*, *20*, 465–477. https://doi.org/10.1016/j.jmapro.2015.06.021

[22] Béchet, E., Cuilliere, J., & Trochu, F. (2002). Generation of a finite element MESH from stereolithography (STL) files. *Computer-Aided Design*, *34*(1), 1–17. https://doi.org/10.1016/s0010-4485(00)00146-9

[23] Ledalla, S. R. K., Tirupathi, B., & Sriram, V. (2016). Performance evaluation of various STL file mesh refining algorithms applied for FDM-RP process. *Journal of the Institution of Engineers (India) Series C*, *99*(3), 339–346. https://doi.org/10.1007/s40032-016-0303-4

[24] Fiberlab S.A. (2022). Technical data sheet - Easy PLA. https://fiberlogy.com/wp-content/uploads/2021/12/FIBERLOGY_EASY_PLA_TDS.pdf (access 16.12.2024)

[25] FreeCAD. Import from STL or OBJ. https://wiki.freecad.org/Import_from_STL_or_OBJ (access 19.02.2025)

[26] Autodesk Inc.. How to export an STL/3MF file from Fusion . https://www.autodesk.com/support/technical/article/caas/sfdcarticles/sfdcarticles/How-to-export-an-STL-file-from-Fusion-360.html (access 19.02.2025)

[27] Fiberlab S.A. (2023). Material safety data sheet - Easy PLA. https://fiberlogy.com/wp-content/uploads/2024/06/FIBERLOGY_MSDS_EASY_PLA.pdf (access 18.02.025)

[28] PN-EN ISO 1101:2017-05. (2017). Geometrical product specifications (GPS) — Geometrical tolerancing — Tolerances of form, orientation, location and run-out

[29] Yang, Y., Wang, T., Chang, Y., Zhang, W., & Cao, M. (2024). Evaluation of Uncertainty in Cylindricity Measurement based on Coordinate Measuring Machine. *Highlights in Science Engineering and Technology*, *107*, 250–253. https://doi.org/10.54097/hdswsh52

[30] Petruse, R. E., Simion, C., & Bondrea, I. (2024). Geometrical and dimensional deviations of Fused Deposition Modelling (FDM) Additive-Manufactured Parts. *Metrology*, *4*(3), 411–429. https://doi.org/10.3390/metrology4030025

[31] Wolf, J., Werkle, K. T., & Möhring, H. (2024). Study on Dynamic Behaviour in FFF 3D-printing with Crossed Gantry Kinematic. *Procedia CIRP*, *121*, 162–167. https://doi.org/10.1016/j.procir.2023.09.244

Paweł Zmarzły received the Ph.D. and D.Sc. from Kielce University of Technology, in 2014 and 2022. He is an Associate Professor and Head of the Metrology Laboratory in the Faculty of Mechatronics and Mechanical Engineering at the Kielce University of Technology. He has authored or co-authored 29 JCR publications and 21 patents and utility model patents. His research activities focus on metrology of geometrical quantities and manufacturing engineering.

Paweł Szczygieł obtained his Bachelor's and Master's degrees in Mechanical Engineering from the Kielce University of Technology in 2020. He is currently a research and teaching assistant at the Kielce University of Technology. His research interests focus on the broad applications of 3D printing in medicine.

Anna Bujarska received the title of Master of Science in Engineering at the Faculty of Computer Management And Modelling of the Kielce University of Technology. Currently a student of the Doctoral School of the Kielce University of Technology in the field of scientific mechanical engineering.